

# Drug Dependent Circadian Variations in AV-nodal Properties During Atrial Fibrillation

Mattias Karlsson<sup>1,2</sup>, Mikael Wallman<sup>1</sup>, Pyotr G Platonov<sup>3</sup>, Sara R. Ulimoen<sup>4</sup>, Frida Sandberg<sup>2</sup>

<sup>1</sup> Dept. of Systems and Data Analysis, Fraunhofer-Chalmers Centre, Gothenburg, Sweden

<sup>2</sup> Dept. of Biomedical Engineering, Lund University, Lund, Sweden

<sup>3</sup> Dept. of Cardiology, Clinical Sciences, Lund University, Lund, Sweden

<sup>4</sup> Vestre Viken Hospital Trust, Bærum Hospital, Rud, Norway

## Abstract

*The heart rate during atrial fibrillation (AF) is highly dependent on the conduction properties of the atrioventricular (AV) node, which can be affected using  $\beta$ -blockers or calcium channel blockers, often chosen empirically. Thus, characterization of the AV nodal conduction properties could contribute to personalized treatment of AF.*

*We have created a mathematical network model of the AV node where continuous estimation of the refractory period and conduction delay from 24-hour ambulatory ECGs from patients with permanent AF ( $n=59$ ) was achieved using a problem-specific genetic algorithm. Circadian variations in the resulting model parameter trends were quantified using cosinor analysis, and differences between treatment with  $\beta$ -blockers and calcium blockers were assessed using a linear-mixed effect approach.*

*The mixed-effects analysis indicated increased refractoriness relative to baseline for all drugs. For the  $\beta$ -blockers, an additional decrease in circadian variation for parameters representing conduction delay was observed. This indicates that the two drug types have quantifiable differences in their effects on AV-nodal conduction properties.*

*The proposed method enables analysis of circadian variation in AV node conduction delay and refractoriness from 24h ambulatory ECG, which can be used to monitor and possibly predict the effect of rate control drugs.*

## 1. Introduction

Atrial fibrillation (AF), which is the most common arrhythmia in the world [1], is characterized by rapid and irregular contraction of the atria arising from a highly disorganized electrical activity [1].

The ventricles are partly shielded from the atrial impulses by the atrioventricular (AV) node, which can block and delay incoming impulses based on its refractory period and conduction delay properties. However, the AV nodal block-

ing is often not sufficient to maintain a healthy heart rate.

To remedy this,  $\beta$ -blockers and calcium channel blockers, two types of rate control drugs, are used to decrease the heart rate by modifying the conduction properties of the AV node [1]. The two drug types affect the AV node in different ways;  $\beta$ -blockers block the  $\beta$ -receptors in AV node cells which reduces the effect of the sympathetic nervous system, and calcium channel blockers prevent the L-type calcium channels from opening which directly modifies the properties of the action potential. Due to these mechanistic differences, responses vary between patients, and the final choice of drug is often made empirically. A non-invasive assessment of the conduction properties of the AV node could potentially give valuable information for better-informed treatment decisions.

Several mathematical models have previously been proposed for characterizing AV node properties. These include models based on invasive data from rabbits [2] and humans [3], and non-invasive data from humans [4]. We have previously proposed an AV node network model capable of assessing the refractory period and the conduction delay of the AV node from 20-minute ECG segments [5].

Using the network model, we propose a framework for 24-hour ECG-based estimation of conduction properties in the AV node comprising a problem-specific genetic algorithm. We use this framework to assess drug-dependent differences in a cohort of 59 patients from the Rate Control in Atrial Fibrillation study [6].

## 2. Network Model of the AV Node

As shown in Figure 1, the network model of the AV node comprises a network of 21 nodes divided into the fast pathway (FP) with 10 nodes, the slow pathway (SP) with 10 nodes, and one coupling node. Each node can either block incoming impulses, depending on its refractory state, or send the impulse to all adjacent nodes with a delay. The refractory period ( $R_j(n)$ ) and the conduction delay ( $D_j(n)$ )

of node  $j$  following an impulse  $n$  are calculated as,

$$R_j(n) = R_{min} + \Delta R(1 - e^{-\tilde{t}_j(n)/\tau_R}) \quad (1)$$

$$D_j(n) = D_{min} + \Delta D e^{-\tilde{t}_j(n)/\tau_D}, \quad (2)$$

where  $\tilde{t}_j(n)$  is the diastolic interval preceding impulse  $n$ ,

$$\tilde{t}_j(n) = t_j(n) - t_j(n-1) - R_j(n-1), \quad (3)$$

and  $t_j(n)$  is the arrival time of impulse  $n$  at node  $j$ . When  $\tilde{t}_j(n)$  is negative, the node is in its refractory state and thus the impulse will be blocked. The parameters  $R_{min}$ ,  $\Delta R$ ,  $\tau_R$ ,  $D_{min}$ ,  $\Delta D$ , and  $\tau_D$  are fixed for all nodes in the SP and the FP, respectively; which results in the 12 model parameters  $\theta = [R_{min}^{FP}, \Delta R^{FP}, \tau_R^{FP}, R_{min}^{SP}, \Delta R^{SP}, \tau_R^{SP}, D_{min}^{FP}, \Delta D^{FP}, \tau_D^{FP}, D_{min}^{SP}, \Delta D^{SP}, \tau_D^{SP}]$ . For the coupling node, the delay is fixed to 60 ms, and its refractory period is fixed to the mean of the ten shortest RR intervals in the data used for model parameter estimation. Furthermore, the input to the model is created using a Poisson process with mean arrival rate  $\lambda$  and the output of the model represents a RR interval series.

### 3. ECG Processing

24-hour ambulatory ECGs from 60 patients during baseline and under the influence of the two calcium channel blockers verapamil and diltiazem and the two  $\beta$ -blockers metoprolol and carvedilol are used in this study [6]. The RR interval series are extracted from the ECGs and the f-waves are extracted using spatiotemporal QRST cancellation [8]. From the f-waves, the AFR trends are estimated using a hidden Markov model-based approach [9]. ECG segments with excessive noise that precluded beat detection and estimation of AFR were excluded from further analysis, resulting in a data set of 270 ambulatory ECG recordings with at least 20-hour duration from 59 patients distributed over baseline and the four treatments.

### 4. Parameter Estimation

The mean arrival rate,  $\lambda$ , is estimated by the AFR trend extracted from the f-waves.

To estimate the model parameters over time, the RR interval series and the  $\lambda$  trends are divided into overlapping data segments corresponding to  $N = 1000$  RR intervals, with a step size of 108 seconds. Thus, each data segment contains one  $\lambda^N(i)$ , calculated as the mean of the  $\lambda$  trend in that segment, and one RR interval series,  $\mathbf{RR}^N(i)$ . The estimated model parameters of the data segment starting at RR interval  $i$  is denoted by  $\hat{\theta}(i)$ .

The Poincaré plot, i.e., a scatter plot of successive RR intervals, is used to quantify the difference between observed and simulated RR series by creating a two-dimensional histogram with a bin width of 50 ms, centered between 250 and 1800 ms. The error function ( $\epsilon$ ) is calculated from the number of samples in the bins according to Equation 4,

$$\epsilon = \frac{1}{K} \sum_{k=1}^K \frac{\left(x_k^N - \frac{N}{N_{sim}} \tilde{x}_k^{N_{sim}}\right)^2}{\sqrt{\frac{N}{N_{sim}} \tilde{x}_k^{N_{sim}}}}, \quad (4)$$

where  $K$  is the number of bins,  $N_{sim}$  is the number of RR intervals simulated with the model, and  $\tilde{x}_k^{N_{sim}}$  and  $x_k^N$  are the numbers of RR intervals in the  $k$ -th bin of the model output and observed data, respectively.

To search for the  $\theta$  yielding the minimum  $\epsilon$ , a problem-specific genetic algorithm (GA) is used. Hyper-parameters in the GA are tuned during the optimization by using the Poincaré difference ( $\Delta P(i)$ ), according to Equation 5,

$$\Delta P(i) = \frac{1}{K} \sum_{k=1}^K \left(x_k^{N_{\Delta P}}(i) - x_k^{N_{\Delta P}}(i+1000)\right)^2, \quad (5)$$

where  $x_k^{N_{\Delta P}}(i)$  and  $x_k^{N_{\Delta P}}(i+1000)$  are the number of RR intervals in the  $k$ -th bin of the Poincaré plot histogram for the RR interval series starting at interval  $i$  and  $i+1000$ , respectively. Here, the number of RR intervals simulated with

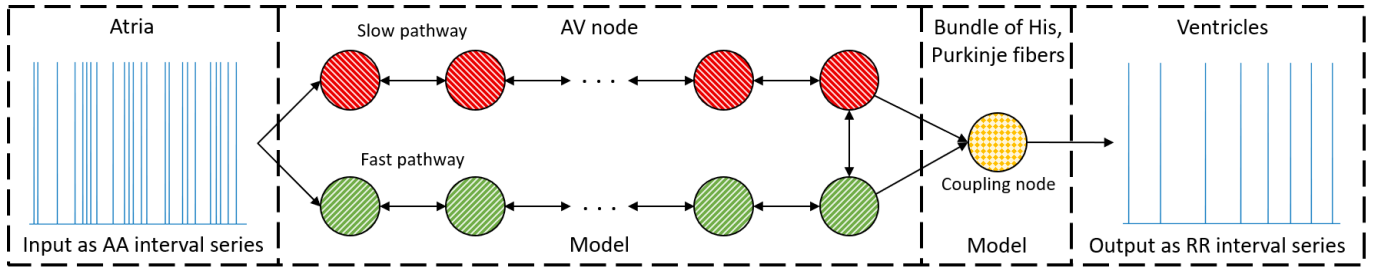


Figure 1: A schematic representation of the network model. The yellow node represents the coupling node, the red nodes the SP, and the green nodes the FP. Furthermore, the arrows indicate the direction for impulse conduction. For enhanced readability, only a subset of the 21 nodes is shown. Adapted from [5].

the model,  $N_{\Delta P}$ , is set to 2000; thus  $\Delta P(i)$  is calculated using 2000 RR interval long segments with 50% overlap.

The population size for the GA used for estimating  $\hat{\theta}(i)$  is 400 individuals, where each individual is a vector of values for  $\theta$ . The GA uses tournament selection, a two-point crossover, and creep mutation.

Based on  $\Delta P(i)$ , the GA runs different numbers of generations before moving to the next data segment; from 1 when  $\Delta P < 800$ ; to 2 when  $800 \leq \Delta P < 2000$ ; to 3 when  $\Delta P \geq 2000$ .

The error function,  $\epsilon$ , varies between realizations due to the stochasticity introduced by the Poisson process used to create the model input. This variation decreases with the length of the simulated RR interval series. However, simulating more RR intervals requires more computing power. Thus,  $N_{sim}$  is set to 1500 in order to have a good balance between computing power and stability.

In the first generation, the individuals are initialized using a latin hypercube sampling in the ranges:  $\{R_{min}^{SP}, R_{min}^{FP}\} \in [150, 650] \text{ ms}$ ;  $\{\Delta R^{SP}, \Delta R^{FP}\} \in [0, 700] \text{ ms}$ ,  $\{\tau_R^{SP}, \tau_R^{FP}\} \in [40, 300] \text{ ms}$ ;  $\{D_{min}^{SP}, D_{min}^{FP}\} \in [0, 30] \text{ ms}$ ;  $\{\Delta D^{SP}, \Delta D^{FP}\} \in [0, 75] \text{ ms}$ ;  $\{\tau_D^{SP}, \tau_D^{FP}\} \in [40, 300] \text{ ms}$ . These values are also used as boundaries for the model parameters, and thus the difference between the upper bound and the lower bound is the range that the parameters can vary within. This range is here denoted  $r(p)$  where  $p$  is the parameter index ordered as in  $\theta$ .

## 5. Circadian Variation

To quantify the drug-dependent circadian variation in the estimated AV node parameters, a linear mixed-effect model is used. The model consists of a 24-hour periodic cosine with

mean  $m$ , amplitude  $a$ , and phase  $\phi$ , as seen in Equations 6, 7, and 8.

$$y_{pat,m}(t) = m_{pat,m} + a_{pat,m} \cos\left(\frac{2\pi}{24}t + \phi\right) \quad (6)$$

$$m_{pat,m} = \alpha + \alpha_m + \eta_{pat} + \eta_{pat,m} \quad (7)$$

$$a_{pat,m} = \beta + \beta_m + \xi_{pat} + \xi_{pat,m} \quad (8)$$

The estimated parameter trends of patient  $pat$  during treatment  $m \in \{\text{Baseline, Verapamil, Diltiazem, Metoprolol, Carvedilol}\}$  is represented by  $y_{pat,m}(t)$ , and  $t$  corresponds to the time of the day, in hours, that  $\hat{\theta}(i)$  relates to. Moreover, the fixed effects for the mean and amplitude during baseline are represented by  $\alpha$  and  $\beta$ , and the fixed effects for the average deviation from baseline caused by the drugs are represented by  $\alpha_m$  and  $\beta_m$ . Furthermore,  $\eta_{pat}$ ,  $\eta_{pat,m}$ ,  $\xi_{pat}$  and  $\xi_{pat,m}$  represents the individual deviation from the fixed-effects, which are assumed to be sampled from a zero-mean gaussian distribution. In addition,  $\alpha_m$ ,  $\beta_m$  and  $\eta_{pat,m}$ ,  $\xi_{pat,m}$  are defined to be zero during baseline. The phase  $\phi$  is assumed to be fixed for the 12 model parameters for each  $\hat{\theta}(i)$  trend and is estimated by principal component analysis, where the phase of the principal component with the highest amplitude is used. With  $\phi$  estimated, all remaining parameters are estimated using the linear mixed-effects model function 'fitlme()' in MATLAB (The MathWorks Inc. version R2019b).

## 6. Results

The fixed effects for the mean,  $\alpha_m$ , and the amplitude,  $\beta_m$ , and their respective 95% confidence interval normalized with  $r(p)$  are shown in Figure 2.

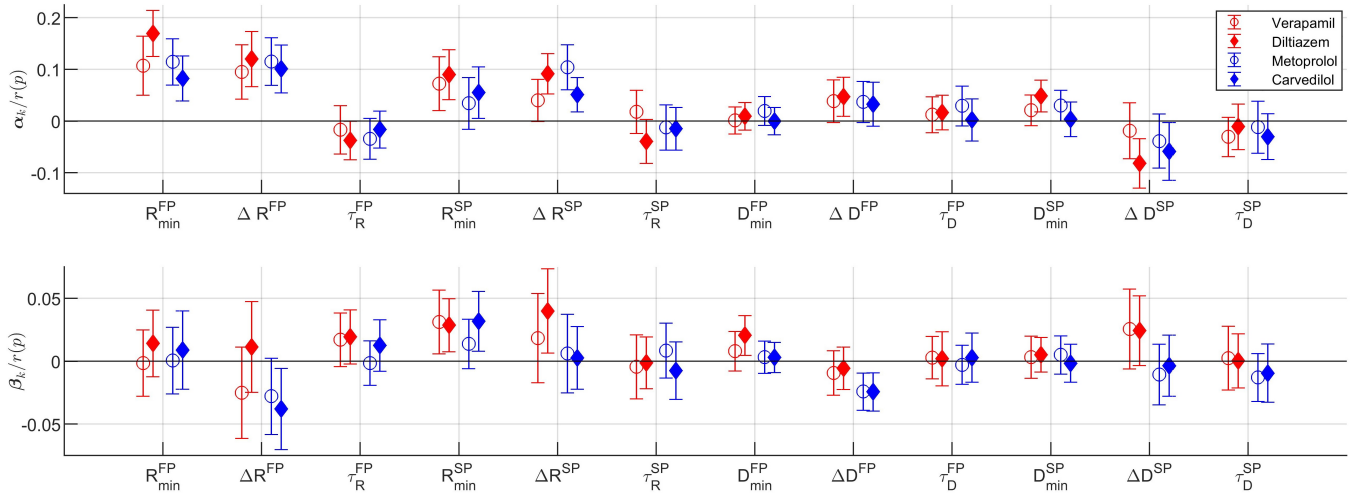


Figure 2: The fixed effects from the linear mixed-effect model with corresponding 95 % confidence intervals for the mean (top) and amplitude (bottom) for each model parameter and drug. [7]

In the figure, top panel, a significant increase ( $p < 0.05$ ) in the mean value is seen for all drugs in  $R_{min}^{FP}$  and  $\Delta^{FP}$ . Furthermore, a significant increase ( $p < 0.05$ ) in either  $R_{min}^{SP}$  or  $\Delta R^{SP}$  is seen for all drugs.

In addition, a distinctly negative effect on the amplitude for  $\Delta D^{FP}$  and  $\Delta D^{SP}$  can be observed for the  $\beta$ -blockers in regards to the calcium channel blockers.

More detailed results about the network model parameters as well as the linear mixed-effect model parameters are found in [7].

## 7. Discussion

The AV node model was originally proposed in [10], and has previously been fitted to twenty-minute ECG segments based on its ability to replicate Poincare plots [5]. The problem-specific GA proposed in the present study enables estimation of model parameters from 24-hour ambulatory ECG recordings and analysis of circadian variation.

The results in Figure 2, top panel, showed a significantly increased refractory period for all drugs relative to baseline in both pathways, which is supported by electrophysiological studies for verapamil, diltiazem, and metoprolol [11–13].

Furthermore, as shown in Figure 2, bottom panel, the circadian variation of the conduction delay (evident by  $\Delta D^{FP}$  and  $\Delta D^{SP}$ ) is decreased for the  $\beta$ -blockers in contrast to the calcium channel blockers. Previously, stimulation of the  $\beta_1$ -receptors, which regulate the autonomic nervous system in the heart, has been shown to increase the conduction velocity in the AV node [14]. Thus, using  $\beta$ -blockers to block these receptors could be assumed to decrease the autonomic nervous system effect, as seen in the results.

A limiting factor in the analysis is the large confidence intervals shown in Figure 2. This is most likely due to high inter-patient variability in parameter values combined with the simplicity of the cosine model and the relatively low sample size of 59 patients. Further, it should be noted that the estimated model parameters are not yet clinically validated for assessment of AV node refractoriness and conduction delay.

## 8. Conclusion

We have presented a mathematical model with an associated parameter estimation framework that enables non-invasive assessment of conduction properties of the AV node over 24 hours. The methodology was applied to ambulatory ECGs from patients with permanent AF during baseline and under the influence of two  $\beta$ -blockers and two calcium channel blockers. Trends in the estimated parameters were described using a linear mixed effects model, identifying differences in the impact on conduction delay between the two drug types.

## References

- [1] Hindricks G, et al. 2020 ESC guidelines for the diagnosis and management of atrial fibrillation developed in collaboration with the european association of cardio-thoracic surgery (EACTS). *Am J Physiol Heart Circ Physiol* 2020;.
- [2] Climent AM, et al. Functional mathematical model of dual pathway AV nodal conduction. *Am J Physiol Heart Circ Physiol* 2011;300(4):H1393–H1401.
- [3] Jørgensen P, et al. A mathematical model of human atrioventricular nodal function incorporating concealed conduction. *Bull Math Biol* 2002;64(6):1083–1099.
- [4] Henriksson M, et al. A statistical atrioventricular node model accounting for pathway switching during atrial fibrillation. *IEEE Trans Biomed Eng* 2015;63(9):1842–1849.
- [5] Karlsson M, et al. Non-invasive characterization of human AV-nodal conduction delay and refractory period during atrial fibrillation. *Front Physiol* 2021;1849.
- [6] Ulimoen SR, et al. Comparison of four single-drug regimens on ventricular rate and arrhythmia-related symptoms in patients with permanent atrial fibrillation. *Am J Cardiol* 2013; 111(2):225–230.
- [7] Karlsson M, Wallman M, Platonov PG, Ulimoen SR, Sandberg F. ECG based assessment of circadian variation in AV-nodal conduction during AF - influence of rate control drugs. *Front Physiol* 2022;13:2015.
- [8] Stridh M, et al. Spatiotemporal qrst cancellation techniques for analysis of atrial fibrillation. *IEEE Trans Biomed Eng* 2001;48(1):105–111.
- [9] Sandberg F, et al. Frequency tracking of atrial fibrillation using hidden markov models. *IEEE Trans Biomed Eng* 2008; 55(2):502–511.
- [10] Wallman M, Sandberg F. Characterisation of human AV-nodal properties using a network model. *Med Biol Eng* 2018;56(2):247–259.
- [11] Leboeuf J, et al. Electrophysiological effects of bepridil and its quaternary derivative cerm 11888 in closed chest anaesthetized dogs: a comparison with verapamil and diltiazem. *Br J Pharmacol* 1989;98(4):1351.
- [12] Talajic M, et al. Rate-dependent effects of diltiazem on human atrioventricular nodal properties. *Circulation* 1992; 86(3):870–877.
- [13] Rizzon P, et al. Electrophysiological properties of intravenous metoprolol in man. *Br Heart J* 1978;40(6):650.
- [14] Gordan R, et al. Autonomic and endocrine control of cardiovascular function. *World J Cardiol* 2015;7(4):204.

Address for correspondence:

Mattias Karlsson  
Chalmers Science Park SE-412 88 Göteborg, Sweden  
Mattias.karlsson@fcc.chalmers.se